X-ray tomography measurements of power-law cluster size distributions for the nonwetting phase in sandstones

Stefan Iglauer,[1,*] Stefano Favretto,[2,†] Gregorio Spinelli,[2,‡] Gianni Schena,[2,§] and Martin J. Blunt[1,‖]
[1]*Department of Earth Science and Engineering, Imperial College London, London SW7 2AZ, United Kingdom*
[2]*Department of Civil Engineering and Environment Engineering, University of Trieste, 34127 Trieste, Italy*
(Received 6 June 2010; published 15 November 2010)

Three-dimensional images of sandstones containing residual nonwetting phase were obtained using synchrotron x-ray tomography with a resolution of approximately 9 μm. We determined the size distribution of disconnected nonwetting phase clusters (ganglia); the number of ganglia of size s is $N(s) \sim s^{-\tau}$ with $\tau = 2.05$. The vast majority of the residual phase was contained in large clusters, spanning many pores. This result implies that we have clusters of all sizes providing a huge surface area for geochemical reactions and dissolution while allowing mobilization of the residual phase during improved oil recovery in hydrocarbon reservoirs and carbon dioxide storage in aquifers.

DOI: 10.1103/PhysRevE.82.056315 PACS number(s): 47.56.+r, 91.60.Np, 47.55.nb, 81.70.Tx

Carbon capture and storage is one method to reduce atmospheric emissions of carbon dioxide (CO_2): CO_2 is collected from the flue gas of power stations or other industrial plants and injected deep underground in porous rock [1]. The principal storage sites are likely to be deep saline aquifers. In the absence of intact extensive caprock, it has been demonstrated that the most rapid way to render the CO_2 immobile, hence preventing escape to the surface, is through capillary trapping: when water displaces CO_2, which is the nonwetting phase, the water preferentially fills the smaller regions of the pore space, surrounding CO_2 such that it can no longer move [2]. We call these disconnected nonwetting phase clusters ganglia.

Capillary trapping will occur at the trailing edge of a CO_2 plume as it migrates upward under gravity, as a result of natural groundwater flow, or can be engineered through the injection of water in addition to CO_2 [3,4]. Simulation studies suggest that capillary trapping can render the vast majority of CO_2 immobile after a few years of water injection [4]. Over hundreds to millions of years, a significant fraction of CO_2 will dissolve in brine and subsequently react with the host rock or brine, forming solid carbonate [5]. The residual saturation—the fraction of the void space occupied by trapped CO_2—determines how much CO_2 can be stored safely underground, while the size distribution of trapped ganglia will control the rate of dissolution and reaction as well as possible remobilization under the influence of viscous and buoyancy forces [5].

Several measurements of the ganglion size distribution have been performed in the literature. In the earliest studies, the nonwetting phase solidified, the rock was dissolved away, allowing ganglia to be observed directly [6]. More recently, x-ray tomography has enabled the pore space and the fluids within it to be imaged directly at a resolution of a few microns [7–10]. These studies have demonstrated that ganglia can range in size from a single pore to multiple-pore structures. The size distribution from these experiments appears to peak at some typical ganglion size and then decay rapidly. Specifically, Prodanović *et al.* [7] observed a size distribution which approximately exponentially increased with a peak at four average pore volumes, a decreasing shoulder, and a sharp cutoff at maximum cluster size (around seven pore volumes). In a glass bead pack, Karpyn *et al.* [10] measured an average cluster size of approximately five pores. The range of cluster size spanned several orders of magnitude, but there was a rapid tailing of the distribution for sizes larger than the average.

In contrast, theoretical and numerical studies hypothesize that trapping is a percolation process, where the wetting phase fills the narrowest regions in order of size, stranding nonwetting phase in the larger pores. The number of ganglia of size s, $N(s) \sim s^{-\tau}$, scales with a universal exponent $\tau = 2.189$ for normal percolation [11]. Displacements in porous media are, however, not a pure percolation process: in particular, there is a competition between cooperative filling of pores that is more akin to an Ising-type model and wetting layer flow that allows narrower regions—throats—to fill in order of size through snapoff [2,12–14]. Furthermore, cooperative filling depends on the contact angle of water in the presence of CO_2 (or oil), with an effective nonzero contact angle affected by roughness of the grain surface, converging and diverging pore geometries, and rock surface chemistry. Despite these complications, simulations on a cubic lattice with cooperative pore filling did observe a power-law ganglion size distribution with $\tau \approx 2.2$ [12]. Hence, the apparent discrepancy between direct measurement and percolation theory is puzzling; in this paper we image the ganglion size distribution to resolve this disagreement.

We selected two sandstone samples: Clashach and Doddington. These are relatively homogeneous porous rocks of different porosities (Table I), and they are representative of reservoir sandstones. We first flooded the cores completely with brine (deionized water doped with 10 wt % potassium iodide to enhance x-ray contrast), then injected 20 pore vol-

*Corresponding author. FAX: +44-2075947444; s.iglauer@imperial.ac.uk
†sfavretto@units.it
‡greg@spinelli.it
§schena@units.it
‖m.blunt@imperial.ac.uk

TABLE I. Properties of the two sandstones.

Specimen	Pores	Average coordination number z	Estimated percolation threshold p_c	Fraction of pore voxels occupied by oil S_{or}	S_{or} measured on larger core samples[a]	Porosity
Clashach	9024	3.10	0.4839	0.3516	~0.37	0.111
Doddington	4135	3.36	0.4464	0.3467	~0.32	0.207

[a]Estimates based on corefloods using the porous plate method [22].

umes of oil (n-octane) at a low capillary number ($N_{cap}=\frac{\mu q}{\sigma}=8.52\times10^{-7}$, where μ is the viscosity, q is the Darcy flow rate, and σ is the interfacial tension) and then injected brine again at a low capillary number ($N_{cap}=1.84\times10^{-6}$) in a secondary imbibition process until no further oil was produced. These low flow rates are typical of likely conditions for CO_2 storage or waterflooding in oil reservoirs and indicate that capillary forces dominate at the pore scale [15]. These specimens were then scanned with synchrotron radiation at the SYRMEP beamline of the Elettra Synchrotron Facility in Trieste, Italy [16] (photon energy=30 keV). We analyzed a subvolume of the resulting images consisting of 300^3 voxels (=19.683 mm^3, nominal resolution of 9 μm). The images were filtered with a $3\times3\times3$ median filter to remove noise [17]. The phases in the images were segmented using Otsu's algorithm [18]. Figure 1 shows images of Clashach sandstone; visually similar results were obtained for Doddington.

First we summed up all the oil voxels to find the residual oil saturation S_{or} and compared these S_{or} values with data measured on similar sandstones [7–9] and our own laboratory measurements on larger core samples (0.0381 m diameter), and we found consistent results (Table I). We then compared S_{or} with the estimated percolation threshold p_c (see Table I). To calculate p_c we needed an estimate of the coordination number z, taking $p_c\cong\frac{3}{2z}$ [19]. While conceptually the void space of the rock can be considered as a lattice of wide pores connected by narrower throats, this topological information is not directly evident from an image. We used a maximum ball algorithm [20] to extract a representative network of pores and throats and compute an average coordination number z. We find that the measured residual saturation is lower than p_c. The discrepancy between p_c and S_{or} is likely to be caused by incomplete wetting and cooperative filling that leads to less trapping than predicted using percolation theory [21]. A more refined estimate for the percolation threshold p_t with trapping $p_t=1-p_c-0.06(z-1)^{-0.60}$ [21] led to even larger estimates of p_t. The z and p_c values determined with the maximum ball algorithm were used to calculate the p_t values.

We then counted the number of oil clusters (ganglia) $N(s)$ of size s voxels. We define a cumulative volume $M(s)=\Sigma_s^\infty sN(s)\sim s^{-\tau+2}$ if we can use percolation theory [12,23–25]. Figure 2 shows $M(s)$ plotted on doubly decadic logarithmic axes. We do not expect to see clusters smaller than a typical pore size, except those detected due to noise or at the edges of the domain. From the network extraction, the typical pore volume $S_{pore}\sim50$ voxels. There is an upper cutoff since we cannot have clusters that are larger than the system size. The largest ganglion has size $S_{max}\approx S_{pores}n^D$, where D is the fractal dimension ≈2.5 [24,26]. n is a typical

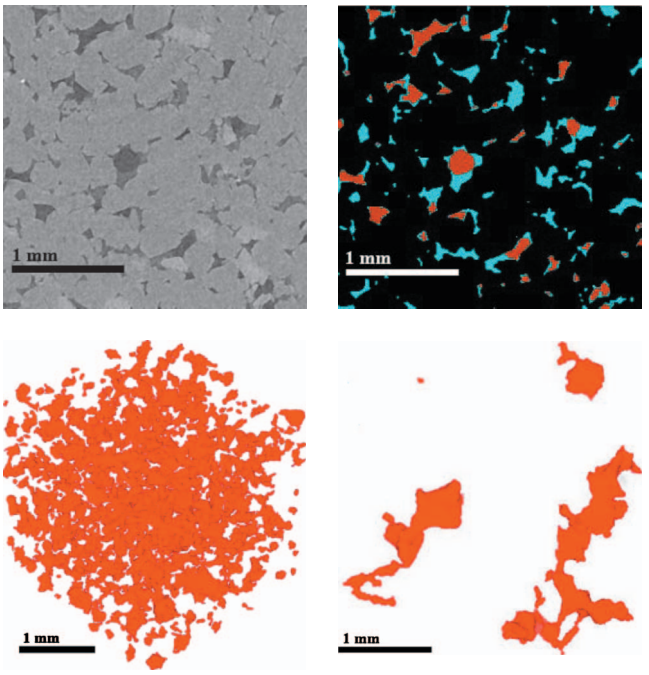

FIG. 1. (Color) Visualization of residual oil in Clashach sandstone after waterflooding. (a) Two-dimensional (2D) grayscale slice: oil is dark, brine is gray, and sandstone is light gray. (b) Segmented 2D image: the area displayed is 300×300 pixels with a nominal resolution of 9 μm. Oil is displayed in red, brine in blue, and rock in brown. (c) Oil only shown in red for a 300^3 voxel image. (d) Individual ganglia of varying size.

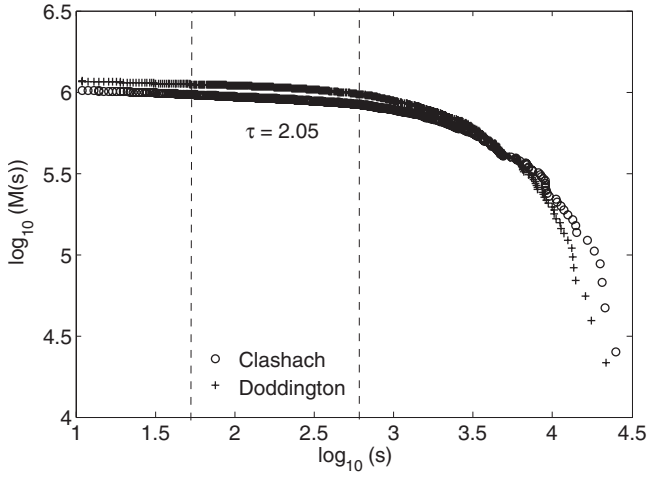

FIG. 2. Base 10 logarithmic cumulant cluster size distribution $\log_{10}(M)$ versus logarithmic cluster size $\log_{10}(s)$. Size s is measured in number of voxels where each voxel has a volume of $(9\ \mu m)^3$.

number of pores across the sample—from Table I this is around 12–20. This gives an estimated $S_{max} \sim 3 \times 10^4 - 9 \times 10^4$, at the lower end of our measured S_{max} of around 3×10^4.

Figure 2 indicates that there is a power-law dependence of $N(s)$ with an exponent slightly lower than −2, over one order of magnitude in s, and with small- and large-scale cutoffs which are physically plausible. Figure 1 visually confirms that we do indeed see clusters that range in size from a single pore to almost spanning the entire system. Recall that s is a volume measure. This contrasts with previous numerical studies where s is a number of trapped pores. As a consequence, our analysis is complicated by the natural variation in effective pore size. Most of the volume of the trapped oil is contained in large ganglia; half the volume is contained in clusters of 60 pores or greater. In contrast, Karpyn *et al.* [10] in a bead pack, which is a more uniform medium, observed fewer large clusters, with half the volume in ganglia smaller than the average pore size.

We fitted a linear least-squares curve through $\log_{10}[M(s)]$ for $\log_{10}(s)$ between 1.7 and 2.8 to obtain $\tau = 2.053 \pm 0.005$ for Clashach and $\tau = 2.053 \pm 0.001$ for Doddington. The total number of clusters N counted in the Clashach sample was 10 538, and 11 718 for Doddington. Our experimental τ (=2.05) is smaller than τ predicted by Monte Carlo simulations ($\tau = 2.189$) for purely random percolation [11] or for percolation with trapping [24]; this could be a consequence of the relatively small system size (equivalent to only 12–20 pores across).

The capillary-controlled displacement of a nonwetting phase by a wetting phase in porous rock is a complex process, involving wetting layer flow and frontal cooperative advance of the fluid interface at an effective contact angle influenced by grain roughness and pore geometry. While the narrower regions of the pore space are preferentially filled by water, it is not surprising that the amount of trapping cannot simply be predicted using an estimated percolation threshold. However, we have shown, using *in situ* imaging, that the distribution of trapped cluster size is a power law with an exponent close to that predicted using percolation theory. This implies that we expect to observe ganglia of all sizes presenting a large surface area for dissolution and reaction in waterflooded oil reservoirs or CO_2 storage sites.

We would like to acknowledge our sponsor Shell under the Shell Grand Challenge on Clean Fossil Fuels and the Elettra Synchrotron Light Source Facility in Trieste, Italy for providing beamtime and technical support.

[1] Working Group III, Intergovernmental Panel on Climate Change (IPCC), *IPCC Special Report on Carbon Dioxide Capture and Storage* (Cambridge University Press, Cambridge, England, 2005).
[2] R. Lenormand, C. Zarcone, and A. Sarr, J. Fluid Mech. **135**, 337 (1983).
[3] R. Juanes, E. J. Spiteri, F. M. Orr, and M. J. Blunt, Water Resour. Res. **42**, W12418 (2006).
[4] R. Qi, T. C. LaForce, and M. J. Blunt, International Journal of Greenhouse Gas Control **3**, 195 (2009).
[5] T. F. Xu, J. A. Apps, and K. Pruess, J. Geophys. Res. **108**, 2071 (2003).
[6] I. Chatzis, N. R. Morrow, and H. T. Lim, SPEJ **23**, 311 (1983).
[7] M. Prodanović, W. B. Lindquist, and R. S. Seright, Adv. Water Resour. **30**, 214 (2007).
[8] M. Kumar, T. J. Senden, A. P. Sheppard, J. P. Middleton, and M. A. Knackstedt, Proceedings of the International Symposium of the Society of Core Analysts, Noordwijk, 2009 (SCA2009-16).
[9] M. Kumar, J. P. Middleton, A. P. Sheppard, T. J. Senden, and M. A. Knackstedt, Proceedings of the International Petroleum Technology Conference, Doha, 2009 (IPTC 14001).
[10] Z. Karpyn, M. Piri, and G. Singh, Water Resour. Res. **46**, W04510 (2010).
[11] C. D. Lorenz and R. M. Ziff, Phys. Rev. E **57**, 230 (1998).
[12] M. J. Blunt, M. J. King, and H. Scher, Phys. Rev. A **46**, 7680 (1992).
[13] M. J. Blunt and H. Scher, Phys. Rev. E **52**, 6387 (1995).
[14] H. Ji and M. O. Robbins, Phys. Rev. B **46**, 14519 (1992).
[15] D. W. Green and G. P. Willhite, *Enhanced Oil Recovery* (SPE, Richardson, 1998).
[16] Elettra Synchrotron Facility (Sincrotrone Trieste), http://www.elettra.trieste.it/
[17] S. Favretto, Ph.D. thesis, University of Trieste, 2009.
[18] N. Otsu, IEEE Trans. Syst. Man Cybern. **9**, 62 (1979).
[19] R. Chandler, J. Koplik, K. Lerman, and J. Willemsen, J. Fluid Mech. **119**, 249 (1982).
[20] H. Dong and M. J. Blunt, Phys. Rev. E **80**, 036307 (2009).
[21] L. Paterson, Phys. Rev. E **58**, 7137 (1998).
[22] C. H. Pentland, Y. Tanino, S. Iglauer, and M. J. Blunt, SPE 133798, *Proceedings of the SPE Annual Technical Conference and Exhibition, Florence* (SPE, Richardson, 2010).
[23] M. Sahimi, *Flow and Transport in Porous Media and Fractured Rock* (VCH, Weinheim, 1995).
[24] M. M. Dias and D. Wilkinson, J. Phys. A **19**, 3131 (1986).
[25] D. Wilkinson, Phys. Rev. A **34**, 1380 (1986).
[26] D. Wilkinson and J. F. Willemsen, J. Phys. A **16**, 3365 (1983).